Journal of Nuclear Materials 401 (2010) 143–148

Contents lists available at ScienceDirect

Journal of Nuclear Materials

journal homepage: www.elsevier.com/locate/jnucmat

Microstructural characterisation and change in a.c. magnetic susceptibility of duplex stainless steel during spinodal decomposition

K.H. Lo [a,b,*], J.K.L. Lai [b]

[a] Department of Electromechanical Engineering, The University of Macau, Macau, China
[b] Department of Physics and Materials Science, City University of Hong Kong, Hong Kong, China

ARTICLE INFO

Article history:
Received 11 November 2009
Accepted 19 April 2010

ABSTRACT

The microstructural changes during long-term (up to 10,000 h) spinodal decomposition in a duplex stainless steel, 7MoPLUS, have been characterised using TEM, a.c. magnetic susceptibility, X-ray diffractometry, microhardness measurement and optical microscopy. The microstructural changes and deformation microstructures of ferrite and austenite upon spinodal decomposition are characterised. The use of a.c. magnetic susceptibility to study the progress of spinodal decomposition is discussed.

Above 450 °C, recent research by K.L. Weng et al. Mater. Sci. Eng. A 379 (2004) 119 [4] has established that spinodal decomposition leads to crisscrossing of dislocations and the development of mottled contrast in the ferrite phase. The present work has shown that at 350 °C (the low-end of the spinodal range), crisscrossing of dislocations still occurs, but mottled contrast is absent. The G phase tends to be in contact with dislocations and its precipitation lags behind the occurrence of spinodal decomposition. No noticeable microstructural changes could be observed in the austenite phase in the spinodal temperature regime.

1. Introduction

The use of the ferritic–austenitic duplex stainless steel (DSS) is extensive nowadays because of their good combination of mechanical and corrosion properties [1]. Their use in the nuclear industry is also increasing. At elevated temperatures, a host of precipitates may form in DSSs, with an attendant degradation in properties [1–3].

In power plants, pipes carrying hot vapour are commonly subjected to temperatures below 550 °C. When ferritic stainless steels containing 15–70%Cr [2] and duplex stainless steels [3,4] are thermally annealed below about 550 °C, their ductility and corrosion resistance are compromised because of spinodal decomposition. During spinodal decomposition, a very fine, coherent, bcc, Cr rich phase (typically denoted as α_{Cr} in the literature and hereafter) will form in the matrix [4–6]. The precipitation of α_{Cr} leads to Cr-depleted regions in the original ferrite matrix. These Cr-depleted regions are denoted α_{Fe} inasmuch as they are enriched with Fe. α_{Cr} embrittles the material as it may hinder dislocation motion. Also, the precipitation of α_{Cr} detracts from corrosion resistance because it leads to Cr-depleted regions in the matrix [4–6].

Changes in mechanical properties [4,5] and magnetic properties [7–11] have been utilised for the monitoring of spinodal decomposition. As regards magnetic properties, Curie temperature [7–9], magnetic coercivity [9], residual induction/magnetisation [9,10], saturation induction/magnetisation [9,10], and remnant ferrite content [11] have all been employed. Nonetheless, the use of a.c. magnetic susceptibility has never been explored as far as the present authors are aware.

Between 600 °C and 950 °C, the intermetallic sigma phase form in the ferrite phase of duplex stainless steels. The a.c magnetic susceptibility has been utilised to probe the precipitation of the sigma phase and its cryogenic magnetic transition (an extensive review on the series of work conducted by the present authors on these topics is in Ref. [3]). The cryogenic magnetic transition of the sigma phase, as indicated by a.c. magnetic susceptibility, has been shown to be useful as a hot-spot indicator [12]. The current work aims to show how this magnetic parameter changes when the DSS, 7MoPLUS, is thermally annealed below 600 °C. Below 600 °C, spinodal decomposition, instead of sigma phase precipitation, prevails.

The aims of the present work were twofold: (1) characterise the microstructural changes and deformation microstructures of the duplex stainless steel, 7MoPLUS, during spinodal decomposition and (2) study the change in a.c. magnetic susceptibility of duplex stainless steel during spinodal decomposition.

* Corresponding author. Address: Faculty of Science and Technology, The University of Macau, Macau (Via Hong Kong), China. Tel.: +853 66688302; fax: +853 28838314.
E-mail address: KHLO@umac.mo (K.H. Lo).

0022-3115/$ - see front matter © 2010 Elsevier B.V. All rights reserved.
doi:10.1016/j.jnucmat.2010.04.014

2. Experimental details

The DSS used in this work was 7MoPLUS from Carpenter Ltd. Its nominal composition is listed in Table 1. The raw material was solution-treated at 1100 °C for 1 h, followed by rapid quenching in iced water. The raw material was in circular bar form (diameter: 25 mm). To study the deformation microstructure, some of the solution-treated material was cold-rolled to 50% reduction in length (from 30 mm in length rolled to 15 mm in length).

To study the spinodal decomposition of the ferrite phase, thermal annealing was conducted at 350 °C, 450 °C, 475 °C, 500 °C and 550 °C for up to 10,000 h. 550 °C was chosen because slightly higher than this temperature, spinodal decomposition would not occur. 350 °C was chosen because microstructural characterisation in this low temperature is seldom reported in the literature.

Magnetic susceptibility measurements were performed using cylindrical samples (diameter: 3 mm, length: 10 mm) that were cut longitudinally from the bar-shaped raw materials. The a.c. magnetic susceptometer was fabricated by the Institute of Physics of the Chinese Academy of Sciences. The susceptometer probe was connected to an SR830 DSP lock-in amplifier from Stanford Research Systems. The internal oscillator of the lock-in amplifier was used to generate sinusoidal excitations to the samples (frequency: 606.0 Hz and amplitude: 1.000 V). The output signals of the susceptometer probe were fed to the lock-in amplifier whose two output channels recorded, respectively, the real and imaginary components of the a.c. susceptibility (in millivolts, mV). The real component is reported in this work. In order to express a.c. magnetic susceptibility in absolute values (in emu/g, e.g.), reference samples of the same dimension as the test pieces with known magnetic moments are required for obtaining the relationship between the mV outputs and the corresponding emu/g values. However, no reference sample was used for establishing the correspondence between mV and emu/g in the current study, insofar as the unit or absolute magnitude of a.c. magnetic susceptibility does not affect the discussions below.

At various stages of annealing, the phases in the samples were identified by using a Siemens D500 X-ray diffractometer (Cu Kα). EDS analyses and microstructural characterisation were done using a Philips CM20 transmission electron microscope.

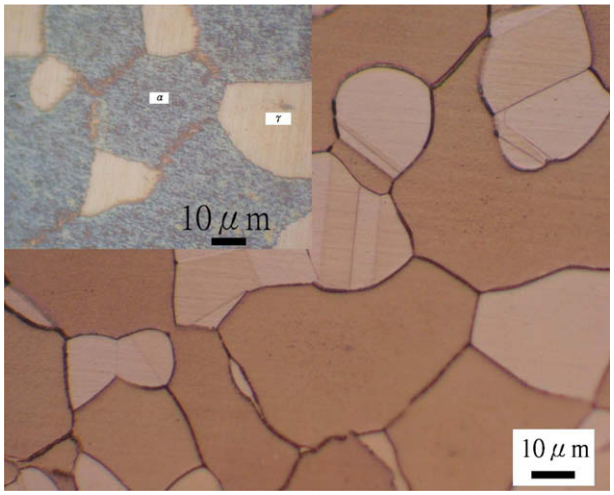

Fig. 1. Microstructure of 7MoPLUS in the as-solution-treated condition (inset: microstructure of a sample that was annealed at 500 °C for 2000 h).

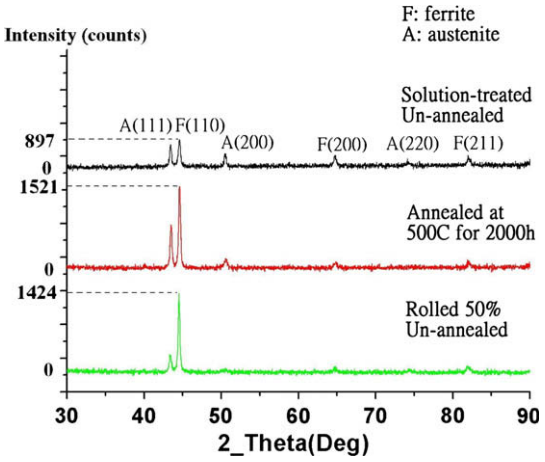

Fig. 2. X-ray diffractograms of variously processed 7MoPLUS.

3. Results and discussions

3.1. Characterisation of solution-treated, unrolled samples

Fig. 1 shows the microstructure of 7MoPLUS in the as-solution-treated state. Image analysis showed that the proportions of ferrite and austenite were about 60% and 40%, respectively. These phase proportions almost remained unchanged for annealing times up to 10,000 h at 500 °C.

Optical microscopy and XRD were unable to reveal clearly the occurrence of spinodal decomposition in the annealed samples. The inset of Fig. 1 shows that the ferrite grain became more susceptible to corrosion attack because the segregation of Cr leads to regions of low-Cr contents. Nevertheless, the structural changes in the ferrite could not be clearly revealed. The XRD diffractograms of unannealed and annealed samples are basically the same (Fig. 2).

However, microhardness measurements did show that the spinodally-decomposed ferrite had been embrittled, whereas the austenite did not harden too much (Fig. 3). The hardness measurements conformed to TEM observations (presented subsequently) which showed that the austenite had remained practically unchanged.

The microstructural changes associated with spinodal decomposition are clearly visible with sample tilting in the TEM. Fig. 4 shows the characteristic mottled contrast [4,13] caused by composition fluctuations associated with Fe and Cr segregations. The figure also shows that a lot of G phase had formed along dislocations.

Fig. 5 is a TEM micrograph of a sample that had been annealed for 10,000 h at 500 °C. It is clear that the edge of the perforation of the sample is not smooth and small globules are visible. At higher magnifications (inset of Fig. 5), globules measuring a few tens nanometres across are clearly revealed. TEM–EDS analyses done in the vicinity of the sample perforation showed an average Cr

Table 1
Nominal composition of 7MoPLUS (wt.%).

Cr	Ni	Mo	Mn[a]	Si[a]	C	N	P[a]	S	Fe
26.0–29.0	3.50–5.20	1.0–2.5	2.0	0.60	0.030	0.15–0.35	0.0350	0.010	Bal.

[a] Maximum value.

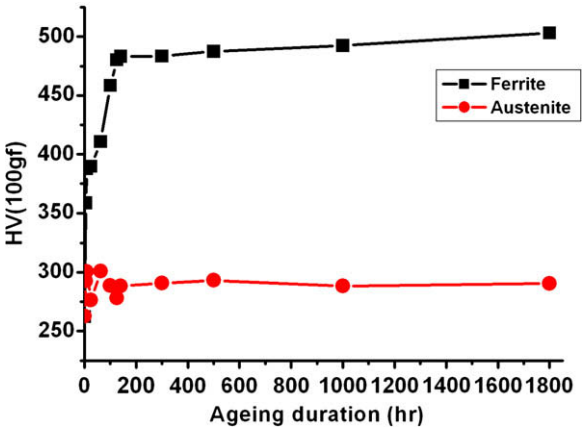

Fig. 3. Hardness changes in the ferrite and austenite phases during spinodal decomposition.

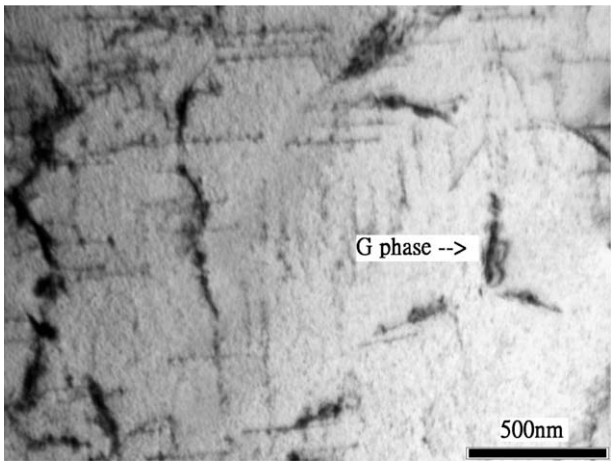

Fig. 4. Mottled contrast caused by composition fluctuations associated with spinodal decomposition in the ferrite phase (annealed at 500 °C for 1744 h).

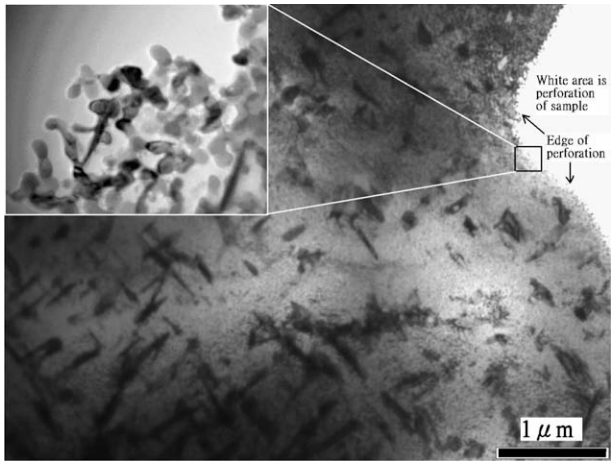

Fig. 5. Globules in the ferrite phase (inset) along the edge of perforation of a TEM sample (annealed at 500 °C for 8000 h).

content of 63.20 wt.%, whereas the Cr content of the sample interior was 23.76 wt.%. It has to be stressed that in the vicinity of the perforation, voids were numerous and the areas selected for EDS analyses were composed of voids and globules. So, the

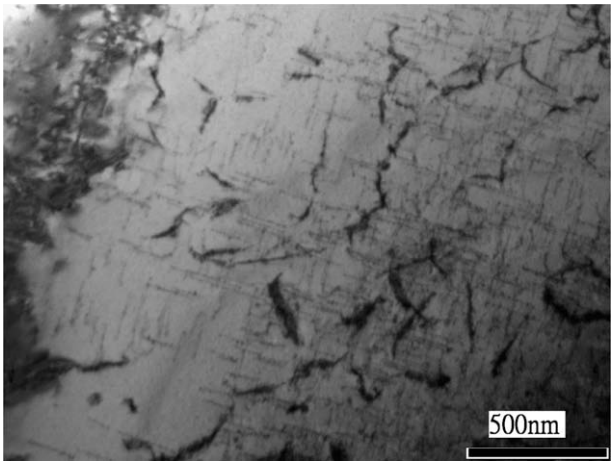

Fig. 6. Crisscrossing of dislocations and the G phase (sample annealed at 500 °C for 1744 h).

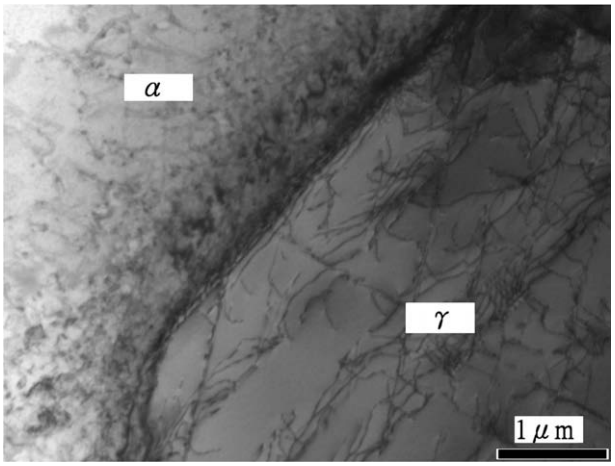

Fig. 7. TEM micrograph of a sample annealed at 500 °C for 8000 h. The austenite grain did not show any appreciable changes.

63.2 wt.% Cr content must not be interpreted as the Cr content of the globules because it is an average value of the Cr contents of voids and globules. The actual Cr contents of the globules are therefore much higher than 63.20 wt.%. Accordingly, because the sample interior is composed of α_{Cr} and α_{Fe}, the actual Cr content of α_{Fe} must be much lower than 23.76 wt.%.

These high-Cr globules are most likely to be α_{Cr} on grounds of their Cr contents. Kuwano and Imamasu [14], using Mossbauer spectrometry, found that the Cr content of the α_{Cr} of a CF3 M cast DSS reached 93 at.%. This further supports the inference that the high-Cr globules in the inset of Fig. 5 are α_{Cr}. Because of it high Cr content, α_{Cr} is very corrosion resistant [14], whereas α_{Fe} is not. So most α_{Fe} would have been corroded away during the twin-jetting process when the TEM sample was prepared. Consequently, the voids in the inset of Fig. 5 are likely to be α_{Fe} and the globules α_{Cr}. For spinodally-decomposed DSSs, α_{Cr} and α_{Fe} have been found to interlock one another [13,15]. Therefore, the inset of Fig. 5 provides a rough visualisation of the way how α_{Cr} and α_{Fe} interlock in the spinodally-decomposed ferrite phase of 7MoPLUS.

Another microstructural feature pertinent to spinodal decomposition is the crisscrossing of dislocations. Fig. 6 shows that as annealing went by at 500 °C, the dislocations gradually crisscrossed each other at approximately 90°. Similar dislocation arrangement was observed by Weng et al. [4] and Miller et al.

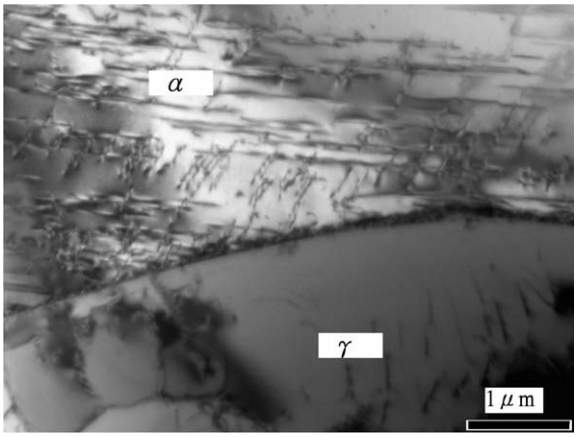

Fig. 8. Both the ferrite and austenite of a sample annealed at 350 °C for 7000 h did not show any changes.

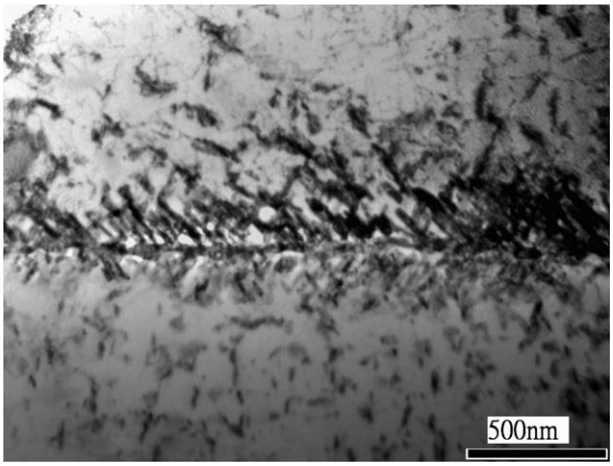

Fig. 9. Precipitates in the vicinity of a ferrite/ferrite boundary of a sample annealed at 500 °C for 1744 h.

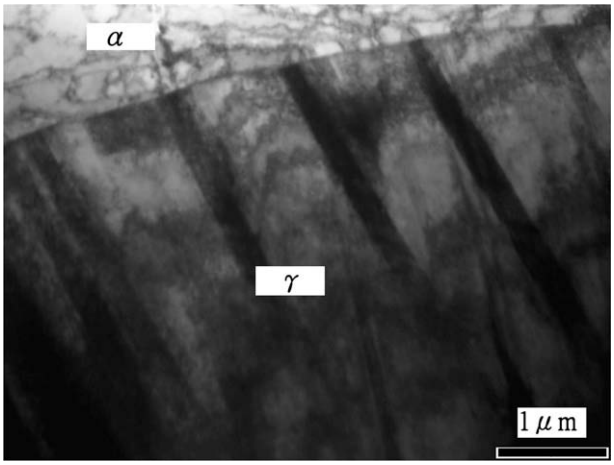

Fig. 10. Uneven distribution of dislocations in slip bands of austenite (50% of reduction in thickness).

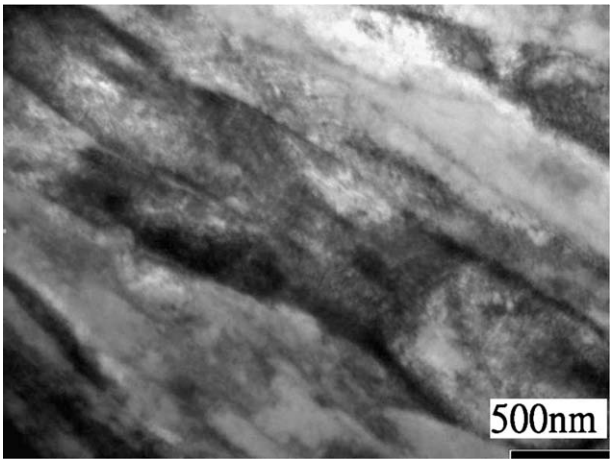

Fig. 11. High dislocation density in the cells of a ferrite grain (50% of reduction in thickness).

[15], too. Weng et al. [4] propounded that such a dislocation arrangement might be partly related to the different coefficients of thermal expansion of ferrite and austenite. These authors also suggested that such a crisscrossing dislocation arrangement contributed to hardening, too, because the dislocations would pin down each other.

In Fig. 6, it is clear that a lot of G phase had formed along dislocations. As regards the austenite phase, it literally underwent no change whatsoever below 500 °C even after prolonged annealing (Fig. 7). This observation conforms to the microhardness measurements of the austenite (Fig. 3).

At 350 °C, spinodal decomposition proceeded extremely sluggishly. Even after annealing for 7000 h, the ferrite did not exhibit any mottled contrast (mottled contrast, on the other hand, was observable for very short times (e.g., a few hours) at 500 °C). It is worth noticing that crisscrossing of dislocations still existed at 350 °C (Fig. 8).

The extremely sluggish rate of spinodal decomposition at 350 °C is understandable because the kinetics of spinodal decomposition follows an Arrhenius-type equation [16]. Hence, the rate of decomposition decreases exponentially with temperature. In fact, it is agreed that study of the annealing behaviour of ferrite below 340 °C is very difficult because of the extremely slow transformation kinetics [16].

As spinodal decomposition proceeded at 500 °C, the G phase formed extensively near grain boundaries (Fig. 9) and those inside the ferrite grains were usually in contact with dislocations (Figs. 4 and 6) as commonly observed [17].

Spinodal decomposition, as evidenced by the mottled contrast, was found to precede the precipitation of the G phase. This conforms to the results of Yamada et al. [18] and the G-phase precipitation model proposed by Mateo et al. [19]. In this model, it is hypothesised that there exists an inter-domain region between α_{Fe} and α_{Cr}. During spinodal decomposition, constituent elements of the G phase are ejected to this inter-domain region. Eventually, this inter-domain region transforms to the G phase when the requisite composition for transformation is reached. According to this model, the G phase must form later than the occurrence of spinodal decomposition. While the mottled contrast indicating spinodal decomposition could be observed under the TEM for annealing at 500 °C for just a few hours, no G phase could be found until annealing for at least a few tens of hours at this temperature. This observation confirms that the G phase only forms at the later stage of spinodal decomposition.

3.2. Characterisation of rolled samples

In the un-annealed condition, rolling produced slip lines in the austenite phase (Fig. 10) and cell-like structure in the ferrite phase (Fig. 11). The cells in the ferrite were of high dislocation density. No

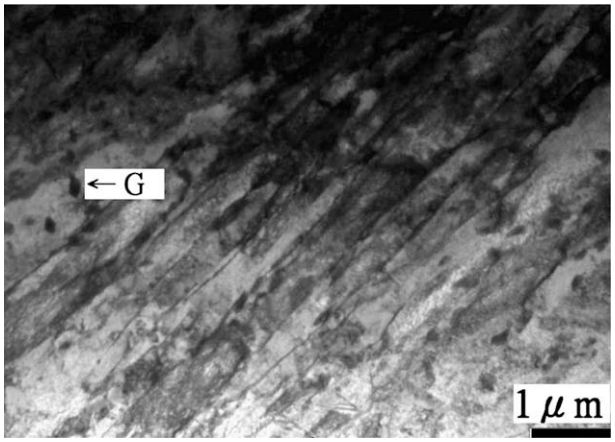

Fig. 12. Cell structure persisted in the ferrite grain of a sample that had been annealed at 500 °C for 10,000 h.

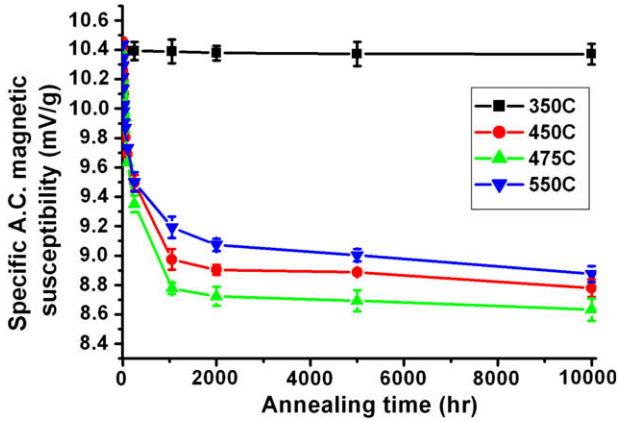

Fig. 13. Changes in the a.c. magnetic susceptibility of samples annealed at different temperatures where spinodal decomposition of the ferrite phase occurs.

deformation-induced martensite could be found in the austenite phase. The dislocation structure of austenite is dependent upon its composition [20,21] and temperature [22], both affect stacking fault energy (SFE). Low SFE promotes planar deformation structures in austenitic stainless steels. Empirical relations have been proposed for the calculation of stacking fault energy (SFE), some of these are as follows (elements in wt.%):

Schramn and Reed [23]:

$$\mathrm{SFE}\ (\mathrm{mJ/m^2}) = -53 + 6.2\mathrm{Ni} + 0.7\mathrm{Cr} + 3.2\mathrm{Mn} + 9.3\mathrm{Mo}$$

Rhodes and Thompson [24]:

$$\mathrm{SFE}\ (\mathrm{mJ/m^2}) = 1.2 + 1.4\mathrm{Ni} + 0.6\mathrm{Cr} + 7.7\mathrm{Mn} + -44.7\mathrm{Si}$$

Spencer [25] and Kruml [26] found planar deformation structures in several 316 austenitic stainless steels. Using the equations above, it may be found that the steels used by these authors possessed higher SFE than the austenite of 7MoPLUS. In addition, nitrogen promotes planar dislocation structure by lowering stacking fault energy [27] (although this viewpoint is disputed by some [28,29]). Inasmuch as the nitrogen content of 7MoPLUS is high (0.6 wt.%) and most of the nitrogen partitions to the austenite phase [1], the planar arrangement of dislocations in the austenite of the rolled samples is reasonable. Planar dislocation structure was also observed in similar DSSs used by Kruml [26] and Marinelli [30]. Occasionally, Marinelli found cell-like structures in the very small austenite in his samples [30]. However, no such cell-like structures could be observed in 7MoPLUS even after a large number of small austenite grains had been examined. Annealing below 500 °C did not alter the dislocation structures of both the ferrite phase and the austenite phase. For example, the cell-like structure in the ferrite phase stayed almost unchanged even after long-term annealing (Fig. 12). The effects of rolling on spinodal decomposition, as reflected by the change in a.c. magnetic susceptibility is presented in the subsequent section.

3.3. Change in a.c. magnetic susceptibility during spinodal decomposition

Fig. 13 shows that as spinodal decomposition progressed, a.c. magnetic susceptibility decreased also. The gradual decrease of a.c. magnetic susceptibility is ascribed to the following two factors: (1) the decomposition of the originally ferromagnetic ferrite α into α_{Fe} (ferromagnetic) and α_{Cr} (paramagnetic) leads to a decrease in the overall ferromagnetism of the duplex stainless steel, and (2) the interlocking morphology of spinodally-decomposed ferrite (inset

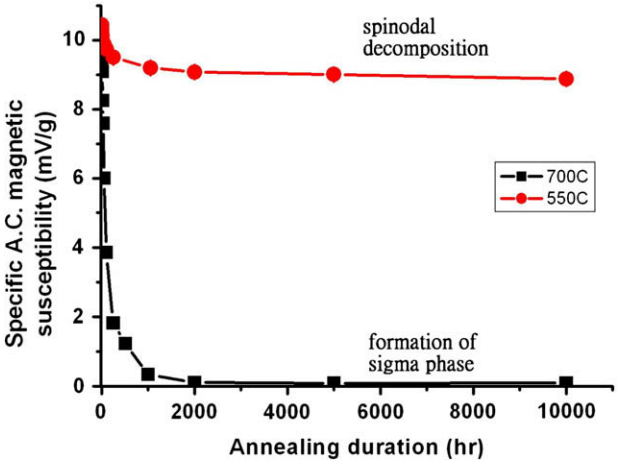

Fig. 14. Changes in a.c. magnetic susceptibility upon annealing at 700 °C where the sigma phase forms and at 550 °C where spinodal decomposition prevails.

of Fig. 5) hinders movement of magnetic domain walls and so the microstructure-sensitive a.c. magnetic susceptibility is decreased [31].

The curves in Fig. 13 drop discernibly at the beginning and then level off (except for the 350 °C curve). This means the rate of spinodal decomposition above 450 °C decreased rapidly at the outset of annealing and then it slowed down as annealing went by. The figure also shows that even after a long time, the a.c. susceptibility curves do not settle to zero, implying incomplete decomposition of ferrite.

The steady state values of the curves corresponding to 450 °C and 550 °C are higher than that of the curve corresponding to 475 °C. This is because spinodal decomposition proceeded more rapidly at 475 °C than at 450 °C and 550 °C.

The curve corresponding to 350 °C is basically flat, signifying that spinodal decomposition was virtually non-existent. The a.c. magnetic susceptibility measurements at 350 °C are very consistent with TEM examination, which showed that that the ferrite was virtually unchanged even after annealing at 350 °C for 7000 h (Fig. 8).

A distinct feature of Fig. 13 is that the a.c. magnetic susceptibility curves do not settle to zero. That is, upon spinodal decomposition, the decomposition of the ferrite phase is incomplete for very long times. This is not the case for precipitation of the sigma phase at higher temperatures. Above 550 °C, the ferrite phase will not

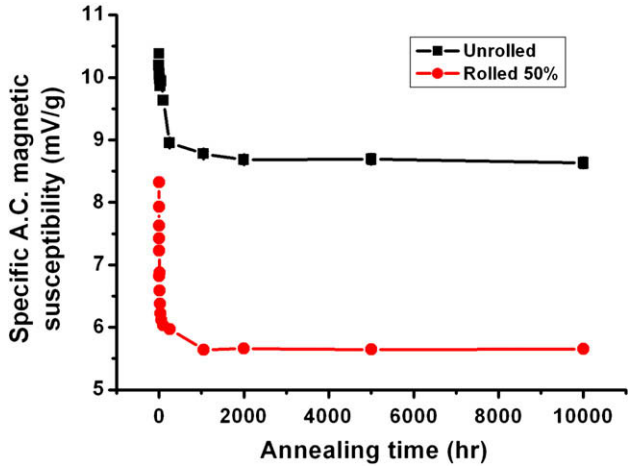

Fig. 15. The effect of rolling on a.c. magnetic susceptibility upon annealing at 475 °C.

decompose spinodally. Instead, it will decompose almost completely into secondary austenite and the intermetallic sigma phase [1–3]. Because both austenite and the sigma phase are paramagnetic at room temperature, a.c. magnetic susceptibility will decrease to zero quickly (Fig. 14). Fig. 14 shows that the a.c. susceptibility curve of a sample that underwent spinodal decomposition (<550 °C) is quite different from that of a sample that formed the sigma phase (between 550 °C and 900 °C). Therefore, if the measured a.c. magnetic susceptibility is nearly zero, then it implies that the duplex stainless steel was previously annealed above 550 °C.

Since dislocations are effective pinning sites of magnetic domains, their increase in number will certainly reduce a.c. magnetic susceptibility. This is indeed the case as demonstrated in Fig. 15. In the unannealed state, rolling reduced the a.c. magnetic susceptibility from about 10.4 mV to 8.3 mV. The profusion of dislocations in the rolled sample facilitates the diffusion of atoms and so spinodal decomposition may proceed more rigorously. In Fig. 15, the drop in a.c. magnetic susceptibility is more rapid in the rolled sample. Also, the pseudo-steady state value of a.c. magnetic susceptibility is lower for the rolled sample, this is because spinodal decomposition is more complete in the rolled sample due to a high dislocation density.

4. Concluding remarks

The microstructural changes (in both the undeformed and deformed states) of the duplex stainless steel, 7MoPLUS, after annealing between 350 °C and 550 °C for up to 10,000 h have been characterised using TEM, a.c. magnetic susceptibility, X-ray diffractometry, microhardness measurement, optical microscopy and image analysis.

A.C. magnetic susceptibility may also be used to differentiate between spinodal decomposition (<550 °C) and the precipitation of the sigma phase (between 550 °C and 900 °C).

It has been established by other authors that when spinodal decomposition occurs at above 450 °C, both mottled contrast (viewed under the TEM) and crisscrossing of dislocations will occur in the ferrite phase. The present work shows that mottled contrast is absent when the annealing temperature drops to about 350 °C, but crisscrossing of dislocations still exists.

The precipitation of the G phase is usually in association with dislocations. And its precipitation lags behind the occurrence of spinodal decomposition, consistent with the model proposed by Mateo et al. [19]. As regards the austenite phase, it virtually exhibits no microstructural changes in the spinodal temperature range.

References

[1] R.N. Gunn, Duplex Stainless Steels: Microstructure, Properties and Applications, Abington Publishing, Cambridge, England, 1997.
[2] J.J. Demo, Handbook of Stainless Steels, in: D. Peckner, I.M. Bernstein (Eds.), McGraw-Hill, 1977.
[3] K.H. Lo, C.H. Shek, J.K.L. Lai, Mater. Sci. Eng. R 65 (2009) 39.
[4] K.L. Weng, H.R. Chen, J.R. Yang, Mater. Sci. Eng. A;poukhvn 379 (2004) 119.
[5] J.K.L. Lai, K.H. Lo, C.H. Shek, D.J. Li, Mater. Sci. Eng. A 406 (2005) 110.
[6] S.S.M. Tavares, V.F. Terra, P. de Lima Neto, D.E. Mateos, J. Mater. Sci. 40 (2005) 4025.
[7] M.R. da Silva, S.S.M. Tavares, D. Fruchart, S. Miraglia, J.M. Neto, J. Magn. Magn. Mater. 226–230 (2001) 1103.
[8] S.S.M. Tavares, P.D.S. Pedrosa, J.R. Teodosio, M.R. da Silva, J.M. Neto, S. Pairis, J. Alloys Compd. 351 (2003) 283.
[9] S.S.M. Tavares, M.R. da Silva, J.M. Neto, J. Alloys Compd. 313 (2000) 168.
[10] S. Evanson, M. Otaka, K. Hasegawa, J. Eng. Mater. Technol. 114 (1992) 41.
[11] J.K.L. Lai, K.W. Wong, Int. J. Press. Ves. Pip. 66 (1996) 325.
[12] J.K.L. Lai, C.H. Shek, K.W. Wong, Acta Mater. 95 (2001) 51.
[13] C.H. Shek, Y.Z. Shao, K.W. Wong, J.K.L. Lai, Scr. Mater. 37 (1997) 529–533.
[14] H. Kuwano, H. Imamasu, Hyperfine Interact. 168 (2006) 1009.
[15] M.K. Miller, J.M. Hyde, A. Cerezo, G.D.W. Smith, Appl. Surf. Sci. 87–88 (1995).
[16] H.M. Chung, Int. J. Press. Vessel. Pip. 50 (1992) 179.
[17] M. Vrinat, R. Cozar, Y. Meyzaud, Scr. Metall. 20 (1986) 1101.
[18] T. Yamada, S. Okano, H. Kuwano, J. Nucl. Mater. 350 (2006) 47.
[19] A. Mateo, L. Llanes, M. Anglada, J. Mater. Sci. 32 (1997) 4533.
[20] X. Dai, A. Wang, X. Cheng, X. Luo, Chin. Phys. 11 (2002) 596.
[21] A.F. Padilha, R.L. Plaut, P.R. Rios, ISIJ Int. 43 (2003) 1350.
[22] R.M. Latanision, A.W. Ruff, Metall. Trans. 2 (1971) 505.
[23] R.E. Schramn, R.P. Reed, Metall. Trans. A 6 (1975) 1345.
[24] C.G. Rhodes, A.W. Thomspson, Metall. Trans. A 8 (1977) 1901.
[25] K. Spencer, J.D. Embury, K.T. Conlon, M. Veron, Y. Brechet, Mater. Sci. Eng. A 387–389 (2004) 873.
[26] T. Kruml, J. Polak, S. Degallaix, Mater. Sci. Eng. A 293 (2000) 275.
[27] P.R. Swan, Corrosion 19 (1963) 102.
[28] L. Vitos, J.O. Nilsson, B. Johansson, Acta Mater. 54 (2006) 3821.
[29] V. Gaviriljuk, Y. Petrov, B. Shanina, Scr. Mater. 55 (2006) 537.
[30] M.C. Marinelli, S. Degallaix, I.A. Armas, Mater. Sci. Eng. A 435–436 (2006) 305.
[31] J. Crangle, Solid State Magnetism, Van Nostrand Reinhold, New York, 1991.